Taylor & Francis
Taylor & Francis Group

Journal of Toxicology and Environmental Health, Part A
Current Issues

ISSN: 1528-7394 (Print) 1087-2620 (Online) Journal homepage: https://www.tandfonline.com/loi/uteh20

Emission of particulate matter from a desktop three-dimensional (3D) printer

Jinghai Yi, Ryan F. LeBouf, Matthew G. Duling, Timothy Nurkiewicz, Bean T. Chen, Diane Schwegler-Berry, M. Abbas Virji & Aleksandr B. Stefaniak

To cite this article: Jinghai Yi, Ryan F. LeBouf, Matthew G. Duling, Timothy Nurkiewicz, Bean T. Chen, Diane Schwegler-Berry, M. Abbas Virji & Aleksandr B. Stefaniak (2016) Emission of particulate matter from a desktop three-dimensional (3D) printer, Journal of Toxicology and Environmental Health, Part A, 79:11, 453-465, DOI: 10.1080/15287394.2016.1166467

To link to this article: https://doi.org/10.1080/15287394.2016.1166467

This article is not subject to US copyright laws

View supplementary material

Published online: 19 May 2016.

Submit your article to this journal

Article views: 5123

View related articles

View Crossmark data

Citing articles: 48 View citing articles

Full Terms & Conditions of access and use can be found at
https://www.tandfonline.com/action/journalInformation?journalCode=uteh20

JOURNAL OF TOXICOLOGY AND ENVIRONMENTAL HEALTH, PART A
2016, VOL. 79, NO. 11, 453–465
http://dx.doi.org/10.1080/15287394.2016.1166467

Taylor & Francis
Taylor & Francis Group

OPEN ACCESS

Emission of particulate matter from a desktop three-dimensional (3D) printer

Jinghai Yi[a], Ryan F. LeBouf[b], Matthew G. Duling[b], Timothy Nurkiewicz[a], Bean T. Chen[b], Diane Schwegler-Berry[b], M. Abbas Virji[b], and Aleksandr B. Stefaniak[b]

[a]Center for Cardiovascular and Respiratory Sciences and Department of Physiology and Pharmacology, West Virginia University School of Medicine, Morgantown, West Virginia, USA; [b]National Institute for Occupational Safety and Health, Morgantown, West Virginia, USA

ABSTRACT

Desktop three-dimensional (3D) printers are becoming commonplace in business offices, public libraries, university labs and classrooms, and even private homes; however, these settings are generally not designed for exposure control. Prior experience with a variety of office equipment devices such as laser printers that emit ultrafine particles (UFP) suggests the need to characterize 3D printer emissions to enable reliable risk assessment. The aim of this study was to examine factors that influence particulate emissions from 3D printers and characterize their physical properties to inform risk assessment. Emissions were evaluated in a 0.5-m^3 chamber and in a small room (32.7 m^3) using real-time instrumentation to measure particle number, size distribution, mass, and surface area. Factors evaluated included filament composition and color, as well as the manufacturer-provided printer emissions control technologies while printing an object. Filament type significantly influenced emissions, with acrylonitrile butadiene styrene (ABS) emitting larger particles than polylactic acid (PLA), which may have been the result of agglomeration. Geometric mean particle sizes and total particle (TP) number and mass emissions differed significantly among colors of a given filament type. Use of a cover on the printer reduced TP emissions by a factor of 2. Lung deposition calculations indicated a threefold higher PLA particle deposition in alveoli compared to ABS. Desktop 3D printers emit high levels of UFP, which are released into indoor environments where adequate ventilation may not be present to control emissions. Emissions in nonindustrial settings need to be reduced through the use of a hierarchy of controls, beginning with device design, followed by engineering controls (ventilation) and administrative controls such as choice of filament composition and color.

ARTICLE HISTORY
Received 19 November 2015
Accepted 13 March 2016

Three-dimensional (3D) printing is used for rapid prototyping and manufacturing in aerospace, defense, and health care. The development of low-cost desktop 3D printers has made these devices widely accessible for small-scale use in business office settings, as well as for personal use in homes and public settings including universities and municipal libraries. There are seven types of 3D printing technologies (Afshar-Mohajer et al., 2015), although most desktop printers use the fused deposition modeling technique in which a heated nozzle melts a solid thermoplastic filament, usually acrylonitrile butadiene styrene (ABS) or polylactic acid (PLA), and deposits multiple thin layers of extruded plastic to form a solid three-dimensional shape (Kim et al., 2015; Stephens et al., 2013). It is well known that office equipment such as laser printers and photocopiers that consume thermoplastic toner powder are emitters of ultrafine particles (UFP, diameter <100 nm) and various chemicals (Destaillats et al., 2008). Given our previous experiences with office equipment as sources of indoor air pollution, there is interest in the potential for emissions from 3D printing technologies that also utilize thermoplastics (Afshar-Mohajer et al., 2015; Kim et al., 2015; Stephens et al., 2013).

Non-manufacturing environments such as offices, homes, classrooms, and libraries are usually designed for occupant comfort, not exposure mitigation. In recent studies, desktop 3D printers were identified as "high emitters" of UFP based upon the categorization scheme developed by He et al. (2007), where release was greater than 10^9 UFP/min while using ABS or

CONTACT Aleksandr B. Stefaniak, PhD, CIH AStefaniak@cdc.gov National Institute for Occupational Safety and Health, Respiratory Health Division, 1095 Willowdale Road, Morgantown, WV 26505, USA.

Color versions of one or more of the figures in the article can be found online at www.tandfonline.com/uteh
Supplemental data for this article can be accessed the publisher's website

Published with License by Taylor & Francis
This article is not subject to US copyright laws
This is an Open Access article. Non-commercial re-use, distribution, and reproduction in any medium, provided the original work is properly attributed, cited, and is not altered, transformed, or built upon in any way, is permitted. The moral rights of the named author(s) have been asserted.

PLA filaments in printers (Kim et al., 2015; Steinle, 2016; Stephens et al., 2013). It is known that there are multiple sources of UFP in non-manufacturing indoor environments, including use of personal appliances and human activities like cooking and burning candles (Schripp et al., 2011; Wallace and Ott, 2011; Wallace et al., 2015). Hence, use of 3D printers in nonmanufacturing or private settings potentially represents another contribution to UFP exposure for indoor workers and the general public to particles with potentially unique physicochemical properties from these other known sources.

Toxicological studies confirmed that UFP penetrate into the alveolar region of the lungs and produce inflammatory responses (Carosino et al., 2015; Oberdorster, 2001), headache (Chang et al., 2015), and cardiovascular effects (Lee et al., 2014; Nurkiewicz et al., 2008). Most desktop 3D printers are not equipped with exhaust ventilation or filtration accessories. Moreover, users in home and public settings typically do not utilize appropriate personal protective equipment, if any. Therefore, it is important to characterize the physicochemical properties of 3D printer emissions to understand exposure potential and risk as early on as possible in the adoption of this technology to non-industrial settings.

The aim of this study was to examine the effects of various factors such as consumables and device design on 3D printer particle emissions to provide information for users to prevent and/or limit exposures. In addition, manufacturers may find data useful for prevention-through-design efforts to minimize emissions.

Methods

Printer-Emission Characterization System and Measurement Instruments

A test chamber was used to generate a real-world emission atmosphere for desktop 3D printers. The chamber system (Figure 1A) consisted of (1) a 500-L stainless-steel chamber to house up to 2 printers for uninterrupted operation; (2) a desktop 3D printer (Replicator 2x®, MakerBot Industries, Brooklyn, NY); and (3) real-time and time-integrated sampling and monitoring instrumentation. The printers sat on a support plate made of a stainless perforated sheet in the chamber. The chamber has eight sampling ports with stainless-steel sampling tubes that extended into the chamber to sample air from the center of the chamber. To accommodate more than eight instruments, flow splitters (TSI Inc., Shoreview, MN) were used during sampling. A two-piece high-efficiency particulate air filter and activated carbon filter (Whatman, Maidstone, UK) was attached to the chamber air inlet to remove particles and organic chemicals, respectively, prior to air entering the chamber. An upward airflow in the chamber was generated when sampling, which eliminated areas of stagnant air in the chamber and resulted in 3D printer emissions being distributed uniformly in this chamber, thereby eliminating bias relative to sampling positions.

Inside the chamber, airborne particle number concentration from 0.02 to 1 μm was measured using a P-Trak (model 8525, TSI Inc.). Particle size and number concentration were measured using instruments that spanned from nanometer to micrometer scale: 0.3 to >20 μm using a GRIMM optical particle counter (model 1.108, GRIMM Aerosol Technik GmbH & Co. Ainring, Germany), 24 nm to 9.38 μm using an electrical low-pressure impactor (ELPI Classic, Dekati Ltd., Tampere, Finland), 14.6 nm to 0.66 μm using a scanning mobility particle sizer (SMPS, model 3910, TSI Inc.), and 0.01 to 0.36 μm using a NanoScan SMPS (model 3910, TSI Inc.). The time resolution of the SMPS and NanoScan SMPS was 2 min to scan 167 size channels and 1 min to scan 13 channels, respectively. Total particle mass concentration was measured using a DustTrak DRX aerosol monitor (model 8534, TSI Inc.). For some print jobs, a real-time instrument was available to measure external particle surface area concentration (model DC 2200 CE, EcoChem Analytics, League City, TX). All instruments were operated at the manufacturer's specified flow rates. A calibrated personal sampling pump was used to collect particles onto polycarbonate filters for off-line electron microscopy analysis. Atmospheric conditions including temperature and humidity inside the chamber were monitored continuously. Conductive carbon tubing and stainless-steel tubing without sharp bends was used as appropriate for sampling; tubing lengths were less than 1 m to minimize

particle line losses (Jankovic et al., 2010). The inlets of the sampling probes were placed approximately 10 cm from the printer.

Test Desktop 3D Printer and Thermoplastic Filaments

For the 3D printer, the filament diameter = 1.75 mm, extruder nozzle diameter = 0.4 mm, and the layer height of extruded plastic = 0.1–0.3 mm. ABS and PLA filaments were tested to investigate the effects of filament type and color on emissions (Table 1). The printer setup for ABS was extruder temperature = 230°C and baseplate temperature = 110°C; while for PLA, extruder temperature = 215°C and the baseplate heater was off.

Sampling Method in a Chamber and a Small Room

Each test consisted of printing one hair comb (Figure 1B). Not all instruments were available for each test and on occasion problems were encountered, such as loss of power, or collected data could not be retrieved from instrument. As such, up to four tests were performed with each filament type and color combination to obtain at least two measurements per instrument. Only one printer nozzle was needed to produce a comb. To investigate the influence of printing with two nozzles, a traffic cone was printed (described in the following). The mass of each printed object was determined gravimetrically using a calibrated microbalance.

For the chamber studies, particle concentrations were measured during the pre-operating (~1 h), printing (~14 min per comb), and post-operating (~1 h) phases. During the pre-operating phase, the chamber was flushed with filtered air until the chamber background particle concentration reached approximately 500 particles/cm^3; then the printer was turned on and the nozzle and baseplate were heated to their set temperatures (no thermoplastic was extruded). No appreciable rise in particle concentration occurred during the nozzle and baseplate heating. Often in testing of laser printers and photocopiers, atmospheric conditions inside a test chamber fluctuate from heat produced by the device and moisture emitted from paper; however, during 3D printing, the conditions inside the chamber were relatively constant with a temperature of

Table 1. Tested filament types and colors.

Filament type	Color 1	Color 2	Color 3	Color 4
ABS	Red	Blue	Natural	Black
PLA	True red	Ocean blue	Transparent blue	Army green

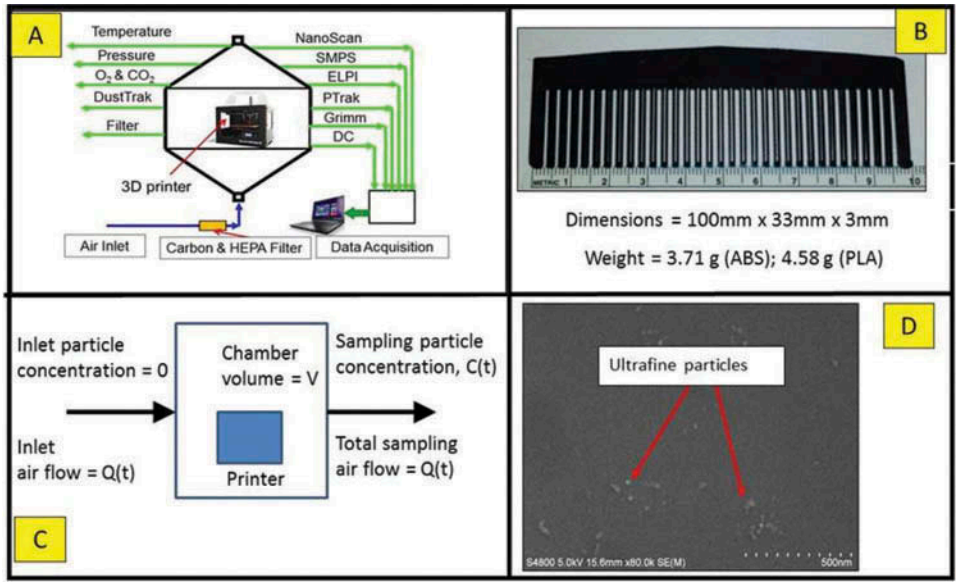

Figure 1. Evaluation of 3D printer emissions: (A) test chamber, (B) print job (hair comb), (C) schematic of emission calculation model, and (D) representative SEM image of emitted particles (ocean blue PLA).

22.1°C and relative humidity (RH) at 35%. The post-operating phase began when the print job ended (printer on, baseplate and nozzle cooling). The total sampling airflow rate was 25 L/min and the chamber air change rate was 3/h.

For the tests in the small room, the inlets of the sampling instruments were placed approximately 10 cm from the 3D printer and measurements were recorded during the pre-printing, printing, and post-printing phases. The small room had a volume of 32.7 m^3 and ambient test conditions were 23.1°C, 26% RH, and 0.974 bar pressure. The air exchange rate in the room was 0.3/h.

Total Particle Emission and Particle Emission Rate

The test chamber utilized is ideally suited for evaluating printer emissions because (1) it prevents particles in the room air from entering into the chamber via a filter attached to the inlet and (2) most particles emitted by the printer are removed from the chamber by sampling airflow (i.e., wall losses are negligible compared to the rate of removal by sampling airflow). Therefore, the total particle (TP) emissions and real-time particle emission rates (PER) can be calculated based on the real-time particle concentration, $C(t)$, recorded by particle monitoring instruments and the total sampling airflow rate, $Q(t)$ (as shown in Figure 1C). The detailed calculation methods for determination of TP and PER are presented in the Supplemental Material.

Statistical Analyses

One-way analysis of variance (ANOVA) models were fitted in JMP version 11.2.0 (SAS Institute, Inc., Cary, NC) to investigate the impact of the fixed effects of color and filament on particle emissions. Tukey's test option was specified for multiple comparisons among colors within a filament type, and Student's *t*-test was used to compare the effect of color (red or blue) between filament types (ABS vs. PLA). ANOVA *F*-statistics were used to note the overall differences in the means of colors within the filament types, while Tukey's test was used to identify specific paired differences between means or red and blue ABS and PLA colors. The criterion for significance was set at $p < .05$.

Results

The average masses (and relative standard deviations) of the printed combs were: 3.64 g (1.95%), 3.71 g (0.03%), 3.65 g (1.72%), and 3.85 g (3.7%) for red, blue, natural, and black ABS, respectively, and 4.50 g (1.75%), 4.65 g (1.58%), 4.56 g (0.29%), and 4.60 g (0.46%) for true red, ocean blue, transparent blue, and army green PLA, respectively. The differences in masses for the same object were attributed to PLA displaying a higher density than ABS (Steinle, 2016).

Reproducibility of Particle Emissions from the Desktop 3D Printer

Responses from all real-time instruments indicated that UFP were emitted during each test. To confirm that the measurements were UFP, not false signals activated by vapor molecules, filter samples of chamber air were analyzed using scanning electron microscopy (SEM). Figure 1D is an example micrograph which indicates that there are many UFP in the printer emissions. Figure 2A is an example plot of real-time SMPS number concentration of the particles emitted by the printer when two combs were printed. Particle concentrations increased rapidly to a peak of approximately 3×10^5 particles/cm^3 a few minutes after printing began and decayed to background approximately 100 min after printing ended. Figure 2B is the SMPS size distributions of the emitted particles. For the first comb, emitted particles had a geometric mean (GM) electrical mobility diameter of 34.7 nm and a geometric standard deviation (σ_g) of 1.4; when printing the second comb, the emitted particles had GM diameter = 32.2 nm (σ_g = 1.5).

Table 2 summarizes the GM particle diameters from SMPS and ELPI measurements when each type and color of filament was utilized. Reproducibility of measurements is evident from the low relative standard deviations (RSD) of particle size measurements (range: 1.4 to 17.6%). Table 3 summarizes calculated values of TP for

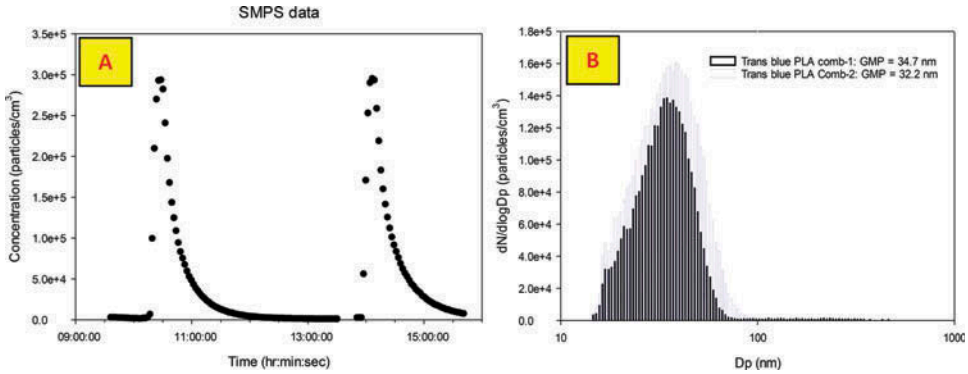

Figure 2. Reproducibility of particle emissions in the chamber for two identical transparent blue PLA combs (SMPS data): (A) number concentrations and (B) size distributions.

Table 2. Average geometric mean (GM) diameters (nm) of emitted particles.

Color/filament	Instrument[a]	Comb 1	Comb 2	Comb 3	Comb 4	Mean	RSD (%)[b]
Natural ABS	SMPS	73.9	66.9	69.6	—[c]	70.1	5.0
	ELPI	53.8	56.7	50.6	—	53.7	5.7
Red ABS	SMPS	66.6	73.9	—	—	70.2	7.3
	ELPI	50.4	49.4	—	—	49.9	1.4
Blue ABS	SMPS	76.6	81.3	—	—	78.9	4.2
	ELPI	62.4	63.1	—	—	63.1	1.7
Black ABS	SMPS	45.2	44.1	—	—	44.6	1.7
	ELPI	45.1	43.5	—	—	45.3	2.0
Army green PLA	SMPS	36.9	37.0	26.0	29.7	32.4	16.9
	ELPI	39.6	31.0	30.8	43.0	36.1	17.1
True red PLA	SMPS	29.1	26.3	27.7	30.0	28.3	5.7
	ELPI	38.5	29.4	35.1	42.7	36.4	15.4
Ocean blue PLA	SMPS	32.2	24.9	25.3	—	27.5	14.9
	GM- ELPI	42.7	32.0	30.0	41.2	36.5	17.6
Transparent blue PLA	SMPS	34.7	32.2	25.7	—	30.1	15.9
	ELPI	40.9	38.7	31.7	39.4	37.7	10.8

[a]SMPS = scanning mobility particle sizer; ELPI = electrical low pressure impactor.
[b]RSD = relative standard deviation.
[c]— = No replicate sample (instrument malfunction or not available).

all tests for all instruments; results indicate generally reliable reproducibility with all colors and types of filaments.

Effects of ABS and PLA Filaments on Particle Emissions

Similar colors of each filament red and blue were compared to evaluate whether filament type influenced emissions. Figure 3 shows the average size distributions (SMPS) of the emitted particles for the whole printing period using true red PLA and red ABS and ocean blue PLA and blue ABS, respectively. Table 2 summarizes the GM electric mobility diameters (SMPS) and GM aerodynamic diameters (ELPI) for these filaments. GM mobility and aerodynamic diameters for red ABS were approximately twofold significantly greater compared to true red PLA. It is of interest that 75% of emitted ABS red particles and more than 99% of emitted PLA true red particles were UFP. Particle GM diameters were significantly larger for blue ABS compared to ocean blue PLA. When printing with blue ABS, approximately 58% of emitted particles were UFP compared to more than 99% for ocean blue PLA. To discern whether the larger particle size observed for ABS particle emissions was the result of agglomeration inside the chamber, the red and blue ABS filaments were measured in a small room; however, data were inconclusive as to how much difference in size may be attributed to agglomeration (results not shown).

Filament type clearly influenced particle emissions. For red ABS and PLA, calculated TP values

Table 3. Total particle (TP) emissions from printing with ABS and PLA filaments.

Color/filament	Instrument[a]	Comb 1	Comb 2	Comb 3	Comb 4	Mean	RSD (%)[b]
Natural ABS	SMPS	2.21×10^{11}	2.33×10^{11}	—	—	2.27×10^{11}	3.7
	ELPI	1.25×10^{11}	2.09×10^{11}	—	—	1.67×10^{11}	35.6
	PTrak	—	—	1.25×10^{11}	2.09×10^{11}	1.38×10^{11}	8.2
	GRIMM	—	—	—	9.74×10^{6}	N/A	N/A
	DustTrak	110.8	249.9	—	—	180.3	54.5
Red ABS	SMPS	2.17×10^{11}	1.61×10^{11}	—	—	1.89×10^{11}	21.0
	ELPI	2.40×10^{11}	2.17×10^{11}	—	—	2.33×10^{11}	7.1
	PTrak	1.59×10^{11}	1.51×10^{11}	—	—	1.55×10^{11}	3.6
	GRIMM	5.26×10^{5}	4.94×10^{5}	—	—	5.10×10^{5}	4.4
	DustTrak	36.9	43.2	—	—	40.1	11.1
Blue ABS	SMPS	1.15×10^{11}	9.43×10^{10}	—	—	1.04×10^{11}	14.0
	ELPI	1.09×10^{11}	—	—	—	N/A	N/A
	PTrak	7.44×10^{10}	5.78×10^{10}	—	—	6.61×10^{10}	17.8
	GRIMM	9.70×10^{5}	9.78×10^{5}	—	—	9.74×10^{5}	0.6
	DustTrak	80.8	75.9	—	—	78.3	4.4
Black ABS	SMPS	1.21×10^{11}	1.69×10^{11}	—	—	1.45×10^{11}	23.4
	ELPI	6.90×10^{10}	7.18×10^{10}	—	—	7.04×10^{10}	2.8
	PTrak	7.41×10^{10}	9.69×10^{10}	—	—	8.55×10^{10}	18.9
	GRIMM	9.20×10^{5}	9.12×10^{5}	—	—	9.16×10^{5}	0.6
	DustTrak	12.7	9.0	—	—	10.9	24.1
Army green PLA	SMPS	2.11×10^{11}	1.45×10^{11}	2.85×10^{11}	—	1.80×10^{11}	18.2
	ELPI	9.67×10^{10}	5.41×10^{10}	4.77×10^{10}	—	6.62×10^{10}	40.3
	PTrak	—	1.53×10^{11}	6.96×10^{10}	—	1.11×10^{11}	50.3
	GRIMM	—	6.43×10^{6}	4.65×10^{6}	7.92×10^{6}	6.33×10^{6}	25.8
	DustTrak	—	31.6	28.5	—	30.1	7.3
True red PLA	SMPS	1.93×10^{11}	2.62×10^{11}	1.09×10^{11}	1.38×10^{11}	1.76×10^{11}	38.4
	ELPI	4.39×10^{10}	3.32×10^{10}	2.36×10^{10}	4.41×10^{10}	3.62×10^{10}	27.1
	PTrak	—	9.53×10^{10}	8.66×10^{10}	5.67×10^{10}	7.95×10^{10}	25.5
	GRIMM	—	5.82×10^{6}	9.18×10^{6}	4.55×10^{6}	6.52×10^{6}	36.7
	DustTrak	—	30.8	44.1	—	37.5	25.1
Ocean blue PLA	SMPS	5.64×10^{10}	2.44×10^{11}	1.67×10^{11}	—	1.56×10^{11}	60.5
	ELPI	2.38×10^{10}	5.83×10^{10}	6.66×10^{10}	2.22×10^{10}	4.27×10^{10}	53.9
	PTrak	—	9.46×10^{10}	7.11×10^{10}	3.02×10^{10}	6.53×10^{10}	49.9
	GRIMM	—	1.13×10^{7}	5.95×10^{6}	1.16×10^{7}	9.62×10^{6}	33.1
	DustTrak	—	60.9	—	54.9	57.5	8.4
Trans. blue PLA	SMPS	2.13×10^{11}	1.93×10^{11}	2.47×10^{11}	—	2.18×10^{11}	12.5
	ELPI	7.77×10^{10}	8.69×10^{10}	4.78×10^{10}	—	7.08×10^{10}	28.9
	PTrak	1.17×10^{11}	2.37×10^{11}	9.76×10^{10}	8.05×10^{10}	1.33×10^{11}	53.3
	GRIMM	—	1.16×10^{7}	5.39×10^{6}	1.06×10^{7}	9.20×10^{6}	36.3
	DustTrak	—	35.4	34.0	—	34.7	2.9

[a]Units are number of particles (SMPS, ELPI, PTrak, GRIMM > 0.65 μm) or micrograms of particles (DustTrak).

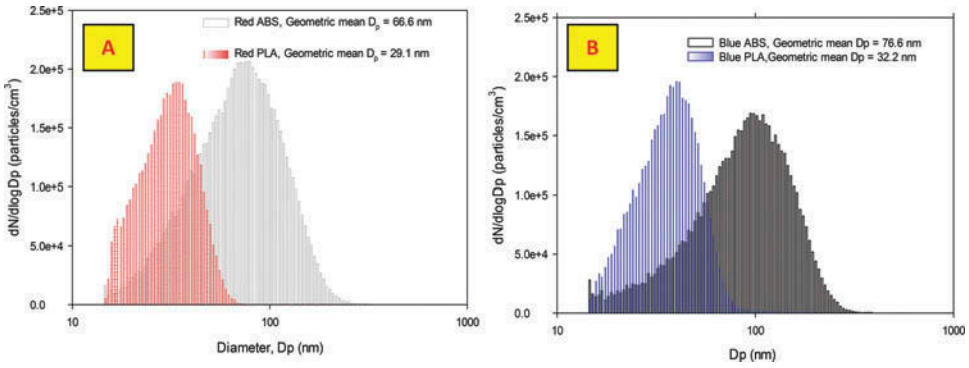

Figure 3. Influence of filament type on size distributions of emitted particles: (A) red ABS and red PLA, and (B) blue ABS and ocean blue PLA.

from ELPI and P-Trak measurements were significantly greater for ABS compared to PLA, although SMPS values were similar. In contrast, TP for particles greater than 0.65 μm (GRIMM) was markedly greater for PLA, although no difference was observed for TP mass. When results were expressed

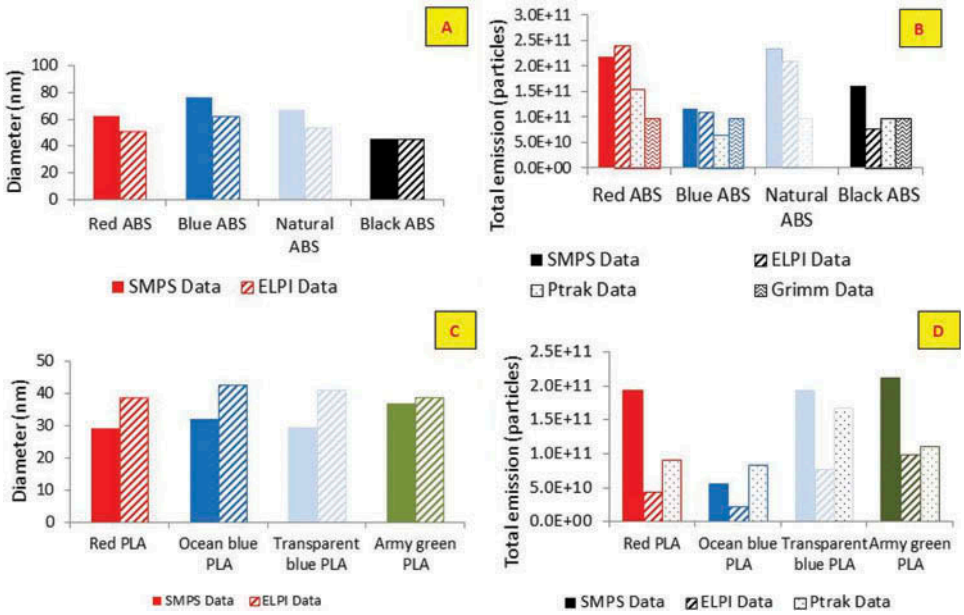

Figure 4. Geometric mean electric mobility (SMPS) and aerodynamic (ELPI) diameters of emitted particles illustrating an influence of filament color on (A) and (C) size, and (B) and (D) total particle emissions.

in terms of yield (TP per mass of printed object) the statistical relationships remained the same. For blue ABS and PLA, there were no marked differences in TP values from SMPS, ELPI, or P-Trak data, although TP for particles greater than 0.65 μm (GRIMM) was significantly higher than for PLA. TP mass (DustTrak) was greater for ABS compared to PLA. On a yield basis, the statistical relationships remained the same except for TP number from the ELPI, which became significantly greater for ABS.

Effects of Filament Color on Particle Emissions

Whether color influenced emissions for a given filament type was determined. Figure 4A shows the GM electric mobility diameters (SMPS) and GM aerodynamic diameters (ELPI) of particles emitted while printing with ABS. Blue ABS emitted the largest particles, which were up to 1.7-fold larger than the size of particles from black (the smallest). GM mobility diameters of blue, red, and natural were markedly larger than black. The GM aerodynamic diameter of blue ABS was significantly larger than for natural, red, or black. As noted earlier, the influence of agglomeration on particle size for ABS emissions in the chamber is unclear. Figure 4B is a plot of TP number emissions from the printer when different colors of ABS filaments were used to print combs. TP number calculated from the SMPS data was significantly higher for natural compared to blue, although differences were not significant for ELPI (red vs. black) or P-Trak results. When one examined particles with size greater than 0.65 μm, it was observed that TP from the GRIMM data was significantly higher for natural compared to red, black, or blue and higher for both blue and black compared to red. The calculated TP mass values from the DustTrak data followed the rank order natural > blue > red > black, although differences were not significant. Expressing data as yield (TP metric normalized to printed ABS filament mass) did not change statistical relationships.

As shown in Figure 4C, GM mobility diameters (SMPS) of PLA-derived particles ranged from 28 nm (red) to 37 nm (army green) and GM aerodynamic diameters (ELPI) were similar (differences not statistically significant). Further, approximately 99% of the emitted particles are UFP regardless of PLA color. Based on the SMPS and ELPI data, when army green PLA was used the printer emitted the highest number of particles (Figure 4D), which was fourfold greater than for ocean blue; P-Trak data showed a similar but less pronounced relationship. The calculated values of TP for particles >0.65 μm were generally similar among PLA colors (Table 3). However, none of the differences among TP number

values from SMPS, ELPI, P-Trak, or GRIMM measurements were significant among colors. TP mass values ranged from 30 (army green) to 58 μg (ocean blue). TP mass for ocean blue was significantly greater than green or transparent blue but not for red. The external surface area of emitted particles for PLA, in μm^2, were (mean (RSD)): 1.22×10^7 (58.8%), 8.68×10^6 (68.8%), 1.17×10^7 (16.9%), and 2.16×10^7 (57.8%) for army green, true red, ocean blue, and transparent blue, respectively and differences were not significant.

Effect of Printer Cover on Particle Emissions

The tested 3D printer has a plastic cover provided by the manufacturer that rests on the top of the device but does not form a tight-fitting seal. Combs in natural ABS color were printed with and without the cover in place in the chamber and in a 32.7-m^3 office. Figures 5A (SMPS) and 5B (ELPI) are plots of the particle number concentrations measurements in the test chamber; the average value of TP from the SMPS was 2.27×10^{11} particles when the cover was on and increased to 4.30×10^{11} particles when the cover was off. The average GM mobility diameter was 70 nm when the cover was on compared to 52 nm when the cover was off, suggesting that some particle agglomeration may occur inside the printer when the cover is on. The ELPI results indicated a similar trend in TP values (average of 1.67×10^{11} with the cover on vs. 5.2×10^{11} particles with the cover off); however, the GM aerodynamic diameters were similar (average of 53.7 nm vs. 57 nm, respectively). P-Trak data were approximately twofold less with the cover on (average of 1.38×10^{11}) versus off (3.3×10^{11}). The TP mass emitted with the cover on was approximately twofold lower than with the cover off (180 μg vs. 328 μg).

Figure S2 is a plot of the real-time particle number concentration measured with a NanoScan SMPS in the office. It is clear that the peak values of the particle number concentrations are 5×10^4 particles/cm^3 and 1.9×10^5 particles/cm^3 when the the cover is on and off, respectively, which is consistent with the chamber test results.

Emissions were also evaluated from a large-scale 3D printer (Dimension series, Stratasys, Eden Prairie, MN) that was manufactured to be housed in a cabinet with a door that would seal and lock closed during printing. The design of the enclosure did not permit us to place our samplers inside the cabinet during printing to measure emissions at the source, although measurements on all instruments in the general room air at a distance of 1 m from the printer did not increase above background (data not shown). The P-Trak and GRIMM were moved to various locations (near the door seams, rear panel, or side) less than 10 cm from the printer and there was no appreciable change in particle number concentration. Hence, sealed enclosures on large-scale 3D printers appear more effective in controlling emissions than loose-fitting covers on cheaper desktop 3D printers.

Effect of Printer Malfunction on Particle Emissions

During one print job with ocean blue PLA filament in the chamber, the desktop 3D printer

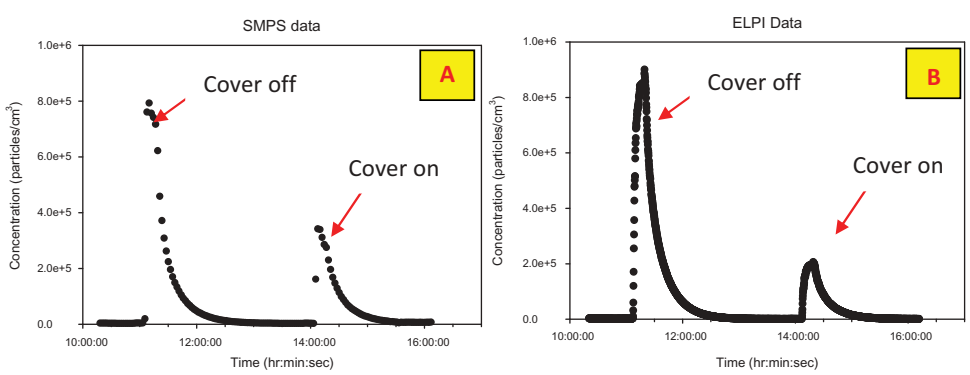

Figure 5. Plots of particle number concentration for the desktop 3D printer in a chamber illustrating an effect of the printer cover on reducing emissions: (A) SMPS and (B) ELPI.

malfunctioned, causing the filament to jam in the heated extruder nozzle, and it was possible to evaluate emissions during this episode and compare levels to those observed during normal operation. The malfunctioning printer emitted higher concentrations of particles compared to normal operation (Figure 6A). From the SMPS, the peak value of the particle concentration from the malfunctioning printer reached 2.8×10^5 particles/cm^3, while the peak value during normal operation was only 8.4×10^4 particles/cm^3. The calculated TP number emitted from the malfunctioning printer (1.24×10^{11} particles) was similar (1.56×10^{11} particles) to normal operation. From the SMPS data, GM mobility diameter was 27.5 nm (σ_g = 1.5) when the printer was malfunctioning and 32.2 nm (σ_g = 1.5) when the printer was operating normally (Figure 6B).

Effect of Two-Nozzle Operation on Particle Emissions

To evaluate the influence of printing with two nozzles compared to one, particle emissions were determined while printing a miniature traffic cone with red and blue ABS in the chamber (Figure 7A). This printing process consisted of 7 sequential steps: (1) red (1.5 min), (2) blue (0.9 min), (3) red (12.1 min), (4) blue (5.75 min), (5) red (4.75 min), (6) blue (4.25 min), and (7) red (4 min) (Figure 7B). The concentration in the chamber immediately rose when the device began printing red for 1.5 min, decreased when printing blue (0.9 min), increased for red (12.1 min), and so on. Corresponding data for the SMPS are shown in Figure 7C. The reason for these peaks and troughs in the profile is that the particle emission rates of the printer are relative to the filament color. The time to print the traffic cone (approximately 34 min) differed from that of the hair comb, so comparisons are more appropriate using PER, which accounts for time. Based on the SMPS measurements from the hair comb printed with one nozzle, PER values are 1.35×10^{10} (red ABS) and 7.43×10^9 (blue ABS) particles/min, while for the traffic cone printed with two nozzles PER value for the entire print job was 6.44×10^9 particles/min.

Figure 7D illustrates the change in particle size distribution with time when printing the traffic cone (SMPS data). When the red base was printed (1.5 min), particle size exhibited a single-mode distribution (59 nm). However, the particle size changed to a bimodal (33 and 130 nm) distribution when the first blue portion of the cone was printed (0.9 min). Subsequently, the GM diameter of the first mode rose from 33 to 55 nm. The increase in size for the first mode suggests that the printing steps involving red ABS only dominated total particle number concentration and that some agglomeration may have occurred. For the hair combs, the printer emitted particles with GM mobility diameters of 70 nm and 79 nm when red and blue ABS filaments were printed individually.

Mean values of PER mass (DustTrak data) were 2.9 ± 0.3 μg/min, 5.6 ± 0.2 μg/min, and 3.4 ± 0.4 μg/min for red (comb), blue (comb), and red and blue (cone) ABS, respectively. The emission rate for blue ABS only was higher than that of red ABS only,

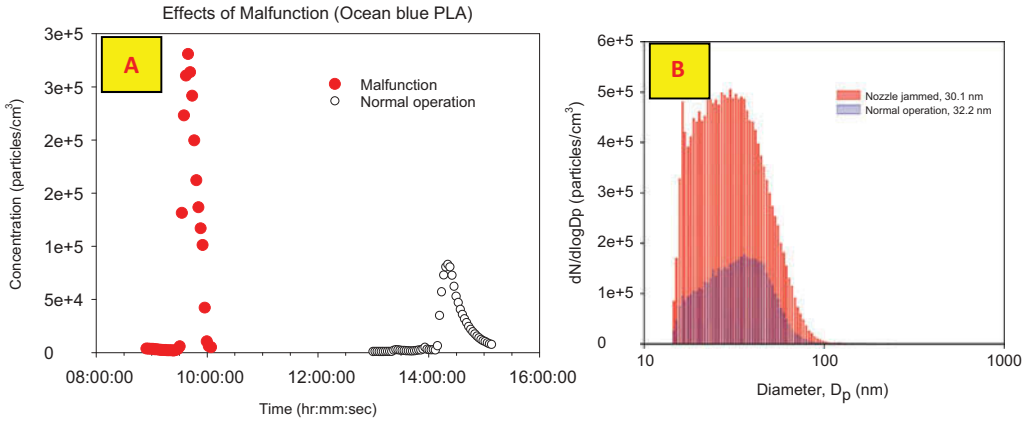

Figure 6. During a malfunction the desktop 3D printer emitted (A) very high concentration of particles compared to normal operation, but (B) particle size was similar.

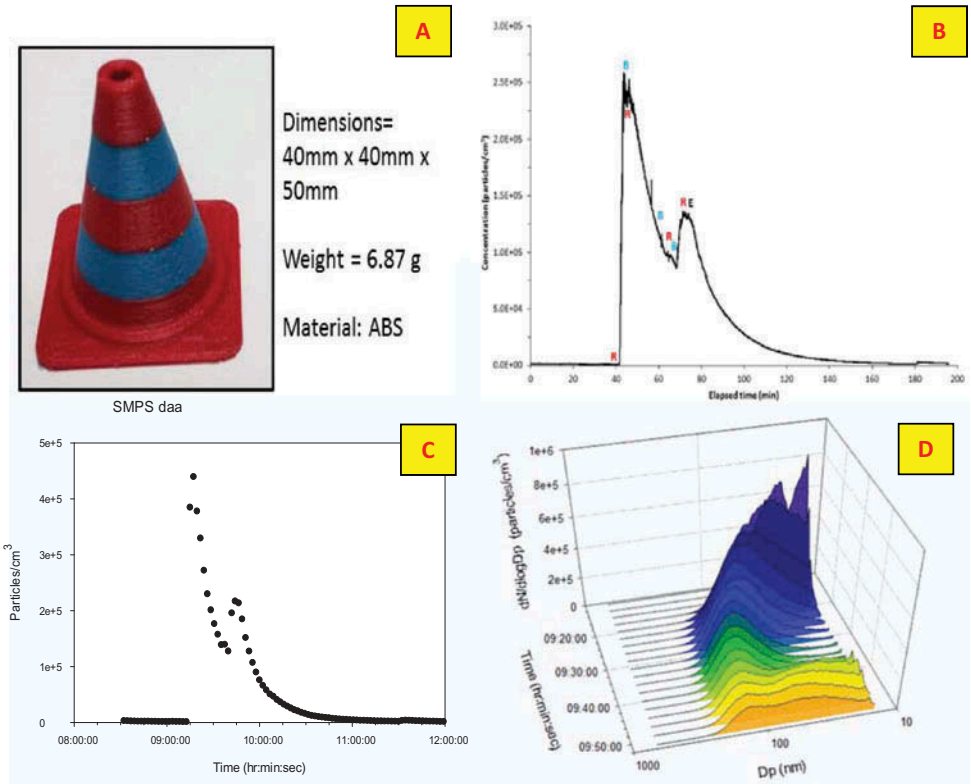

Figure 7. Effect of printing with two nozzles: (A) printed traffic cone, (B) particle number concentration (P-Trak) illustrating changes with the printing sequence (R = start printing red, B = start printing blue, E = end of print job), (C) particle number concentration (SMPS), and (D) changes in particle size distributions with time.

consistent with the larger emitted particle size; however, when both colors were used to extrude the traffic cone, the mass emission rate was intermediate.

Discussion

Desktop 3D printers use a heated nozzle to melt a solid thermoplastic filament. During this process, filament polymers and additives may react with oxygen, resulting in particulate emissions from by-products formed during heating (Contos et al., 1995). The greater the difference between the extruder (ABS, 230°C; PLA, 215°C) and filament melting temperatures (ABS, 105°C; PLA, 150°C), the more vapor can be generated and condense to form UFP by gas-to-particle conversion via nucleation and/or condensation processes. For ABS the temperature difference is 125°C and for PLA it is only 65°C. Thus, particle emissions from ABS are expected to be higher than PLA. Our results demonstrated higher TP number (ELPI, P-Trak) for red ABS compared to red PLA and higher TP mass for blue ABS compared to ocean blue PLA; however, TP number of larger particles (GRIMM) was higher for red and ocean blue PLA (Table 3). Similar to our ELPI and P-Trak data, previous reports (Kim et al., 2015; Stephens et al., 2013) observed higher TP number from ABS relative to PLA, although Steinle (2016) noted that a PLA filament had a higher particle number emission rate in a chamber. The primary sources of 3D printer emissions are likely the heated components, that is, extruder nozzles and baseplate. PLA is a biodegradable polymer manufactured out of plant-based resources such as corn starch or sugar cane. ABS is synthesized from oil-based resources (Weinhoffer, 2012). Our results affirm the findings of previous studies that total emissions and rates differ between ABS and PLA (Afshar-Mohajer et al., 2015; Kim et al., 2015; Steinle, 2016; Stephens et al., 2013). Further, data show that emissions from a 3D printer differed by color within and between types of filaments. It is

postulated that within a given filament type (ABS or PLA) the observed variability may be attributed to the additives used to impart color. Unlike laser printers, which blend three basic colors of toner to create new colors, with fused deposition printers the filament colors cannot be blended so each possesses specific additives (e.g., transition metals) to impart unique color. Between filament types, differences in emissions are likely because of unique additives used to impart color, as well as differences in extrusion temperatures as noted earlier.

A useful parameter for comparing emission results among studies is particle yield because this parameter is independent of print time and object size. Yield can be defined as the ratio of a particle emission metric (number, mass, surface area) to the mass of filament consumed or the mass of the printed object (Kim et al., 2015; Steinle, 2016). Table S1 summarizes UFP number yield for this study and published literature based on SMPS measurements. When emissions were normalized to printed or consumed filament mass, number yields from our study were generally similar between ABS and PLA. Kim et al. (2015) reported a higher yield for a red ABS compared to a brown PLA, but Steinle (2016) noted the reverse relationship. Hence, a clear and consistent relationship between filament type and emissions is difficult to discern from limited published data available.

The design characteristics of the 3D printer itself might influence emissions. The cover of this desktop 3D printer reduced the volume of air in which emitted particles occupied and may have resulted in an increase in coagulation and/or deposition of particles on the inside walls of the printer (as seen by the rise in mobility particle size to 62 nm and decrease in TP number from the SMPS data). If the extruder nozzle jams, the thermostat for the printer continues to heat the nozzle and heat is not transferred to the filament as efficiently as when the printer is in normal operation, which results in an elevated quantity of emissions (Figure 6). Collectively, these design factors have practical implications, as it is likely that when a jam occurs, the first thing a user will do is remove the cover to investigate the problem. Such an action may result in higher exposures than during normal operation. Hence, it is prudent to not open the door or lift the cover off of a 3D printer immediately when a filament jam occurs. A prevention-through-design modification to current device designs would be an automated shutoff for the nozzle heater in the event of a jam.

Implication of 3D Printer Emissions for Human Health

Exposure to small particles has important health implications. Epidemiological studies indicate that exposure to ambient PM is associated with increased respiratory and cardiovascular morbidity and mortality rate (Costa et al., 2014; Lee et al., 2014; Stojic et al., 2016), with effects being pronounced in children (Gauderman et al., 2015) and the elderly (Simoni et al., 2015). Inhaled UFP are deposited throughout the respiratory tract (Oberdorster et al., 2005), may traverse through different protective barriers into the bloodstream (Oberdorster, 2001), and lead to injuries of the respiratory and other organ systems. Deposition of UFP in the nasal and tracheobronchial regions is also important because these regions contain nerve endings that link to the central nervous system; the olfactory neuronal pathway is efficient for translocating inhaled UFP such as fullerenes (Oberdorster, 2004) and manganese oxide (Elder et al., 2006), which result in adverse effects in the brain.

In a risk assessment of UFP emitted by laser printers, particle number best described epidemiological risk (Hänninen et al., 2010). In that study, alveolar deposition of 1.1 to 3.1 $\times 10^9$ particles/d correspond to 12 (home use) to 34 (office use) deaths/10^6 persons, which was deemed to be lower than the estimated risk for exposure to ambient PM. The regional lung deposition and uptake of alveolar deposited UFP was modeled for the largest (ABS blue) and smallest (PLA true red) measured size distributions (Table S2). UFP emitted by the 3D printer are predicted to deposit throughout the regions of the respiratory tract: 5–11% (extrathoracic), 8–17% (tracheobronchial), and 12–34% (alveolar). As noted earlier, deposition of UFP in the head and conducting airways also has implications for health effects. Calculated alveolar uptake of UFP ranged from 2.9 (blue ABS) to 9.7×10^7 (red PLA) particles, which is two orders of magnitude lower than calculated for laser printers. While these initial calculations suggest less risk from 3D

printers, caution needs to be taken in their interpretation. For purposes of comparison, the same estimates of printing time were used as used by Hänninen et al. (2010), although 3D print jobs last several minutes to hours whereas printing on paper tends to require seconds to minutes, and thus it is likely that our exposure estimates are biased low. Further, these risk values do not consider children whose lung development is affected by exposure to ambient PM (Gauderman et al., 2015) or susceptible elderly populations (Simoni et al., 2015), and hence these populations may be more sensitive to high numbers of 3D printer emissions in homes where adequate ventilation is often lacking. Finally, 3D printers likely also emit chemicals during heating of the filament, and whether risk estimates derived from laser printer UFP emissions are applicable to mixed emissions from 3D printers in workplaces and homes is still not fully understood.

Conclusions

Desktop 3D printers might emit high numbers of ultrafine and fine particles during operation. Emissions are influenced by the consumables, including filament type and color, as well as by the printer design characteristics. Exposure to high concentrations of UFP particles emitted from laser printers has been associated with increased risk in mortality frequency, but whether such risks apply to emissions from 3D printers is yet to be elucidated. Based upon our data, evidence indicates that it is prudent to recommend the following precautions to reduce exposures in non-industrial workplaces as well as public locations such as in libraries or universities and private homes: (1) Always use the manufacturer's supplied controls (full enclosure appears more effective at controlling UFP emissions than a cover); (2) use the printer in a well-ventilated place, and/or directly ventilate the printer; (3) maintain a distance from the printer to minimize breathing in emitted particles and choose a low-emitting printer and filament when possible; (4) if the printer nozzle jams, turn off the printer and allow it to ventilate before removing the cover; and (5) utilize the industrial hygiene hierarchy of controls to mitigate exposures (from most to least preferable): engineering > administrative > protective equipment (e.g., respirators).

Acknowledgments

Mention of a specific product or company does not constitute endorsement by the Centers for Disease Control and Prevention. The findings and conclusions in this report are those of the authors and do not necessarily represent the views of the National Institute for Occupational Safety and Health. The authors thank R. Lawrence and A. Johnson for assistance with the data collection and Drs. Antonini and Ku at NIOSH for critical review of this article.

Funding

This work was funded by a NIOSH-intramural National Occupational Research Agenda (NORA) grant as well as NIH-R01-ES015022 (TRN), and NSF-DGE-1144676 (TRN). None of the funding sources had a role in the conduct of the research, study design, data collection analysis or interpretation, or the decision to publish this work.

Conflict of Interest

The authors declare that they have no actual or potential competing interests, financial or otherwise.

References

Afshar-Mohajer, N., Wu, C. Y., Ladun, T., Rajon, D.A., and Huang, Y. 2015. Characterization of particulate matters and total VOC emissions from a binder jetting 3D printer. *Build. Environ*. 93: 293–301.

Carosino, C. M., Bein, K. J., Plummer, L. E., Castaneda, A. R., Zhao, Y., Wexler, A. S., and Pinkerton, K. E. 2015. Allergic airway inflammation is differentially exacerbated by daytime and nighttime ultrafine and submicron fine ambient particles: Heme oxygenase-1 as an indicator of PM-mediated allergic inflammation. *J. Toxicol. Environ. Health A* 78: 254–266.

Chang, C. C., Chiu, H. F., and Yang, C. Y. 2015. Fine particulate air pollution and outpatient department visits for headache in Taipei, Taiwan. *J. Toxicol. Environ. Health A* 78: 506–515.

Contos, D. A., Holdren, M. W., Smith, D. L., Brooke, R. C., Rhodes, V. L., and Rainey, M. L. 1995. Sampling and analysis of volatile organic compounds evolved during thermal processing of acrylonitrile butadiene styrene composite resins. *J. Air Waste Manage. Assoc*. 45: 686–694.

Costa, S., Ferreira, J., Silveira, C., Costa, C., Lopes, D., Relvas, H., Borrego, C., Roebeling, P., Miranda, A. I., and Teixeira, J. P. 2014. Integrating health on air quality assessment—Review report on health risks of two major European outdoor air pollutants: PM and $NO_{(2)}$. *J. Toxicol. Environ. Health B* 17: 307–340.

Destaillats, H., Maddalena, R.L., Singer, B. C., Hodgson, A. T., and McKone, T. E. 2008. Indoor pollutants emitted by

office equipment: A review of reported data and information needs. *Atmos. Environ*. 42: 1371–1388.

Elder, A., Gelein, R., Silva, V., Feikert, T., Opanashuk, L., Carter, J., Potter, R., Maynard, A., Ito, Y., Finkelstein, J., and Oberdorster, G. 2006. Translocation of inhaled ultrafine manganese oxide particles to the central nervous system. *Environ. Health Perspect*. 114: 1172–1178.

Gauderman, W. J., Urman, R., Avol, E., Berhane, K., McConnell, R., Rappaport, E., Chang, R., Lurmann, F., and Gilliland, F. 2015. Association of improved air quality with lung development in children. *N. Engl. J. Med*. 372: 905–913.

Hänninen, O., Brüske-Hohlfeld, I., Loh, M., Stoeger, T., Kreyling, W., Schmid, O., and Peters, A. 2010. Occupational and consumer risk estimates for nanoparticles emitted by laser printers. *J. Nanopart. Res*. 12: 91–99.

He, C., Morawska, L., and Taplin, L. 2007. Particle emission characteristics of office printers. *Environ. Sci. Technol*. 41: 6039–6045.

Jankovic, J. T., Hall, M. A., Zontek, T. L., Hollenbeck, S. M., and Ogle, B. R. 2010. Particle loss in a scanning mobility particle analyzer sampling extension tube. *Int. J. Occup. Environ. Health* 16: 429–433.

Kim, Y., Yoon, C., Ham, S., Park, J., Kim, S., Kwon, O., and Tsai, P. J. 2015. Emissions of nanoparticles and gaseous material from 3D printer operation. *Environ. Sci. Technol*. 49: 12044–12053.

Lee, B. J., Kim, B., and Lee, K. 2014. Air pollution exposure and cardiovascular disease. *Toxicol. Res*. 30: 71–75.

Nurkiewicz, T. R., Porter, D. W., Hubbs, A. F., Cumpston, J. L., Chen, B. T., Frazer, D. G., and Castranova, V. 2008. Nanoparticle inhalation augments particle-dependent systemic microvascular dysfunction. *Part. Fibre Toxicol*. 5: 1.

Oberdorster, E. 2004. Manufactured nanomaterials (fullerenes, C60) induce oxidative stress in the brain of juvenile largemouth bass. *Environ. Health Perspect*. 112: 1058–1062.

Oberdorster, G. 2001. Pulmonary effects of inhaled ultrafine particles. *Int. Arch. Occup. Environ. Health* 74: 1–8.

Oberdorster, G., Oberdorster, E., and Oberdorster, J. 2005. Nanotoxicology: An emerging discipline evolving from studies of ultrafine particles. *Environ. Health Perspect*. 113: 823–839.

Schripp, T., Kirsch, I., and Salthammer, T. 2011. Characterization of particle emission from household electrical appliances. *Sci. Total Environ*. 409: 2534–2540.

Simoni, M., Baldacci, S., Maio, S., Cerrai, S., Sarno, G., and Viegi, G. 2015. Adverse effects of outdoor pollution in the elderly. *J. Thoracic Dis*. 7: 34–45.

Steinle, P. 2016. Characterization of emissions from a desktop 3D printer and indoor air measurements in office settings. *J. Occup. Environ. Hyg*. 13: 121–132.

Stephens, B., Azimi, P., El Orch, Z., and Ramos, T. 2013. Ultrafine particle emissions from desktop 3D printers. *Atmos. Environ*. 79: 334–339.

Stojic, S. S., Stanisic, N., Stojic, A., and Sostaric, A. 2016. Single and combined effects of air pollutants on circulatory and respiratory system-related mortality in Belgrade, Serbia. *J. Toxicol. Environ. Health A* 79: 17–27.

Wallace, L., and Ott, W. 2011. Personal exposure to ultrafine particles. *J. Expos. Sci. Environ. Epidemiol*. 21: 20–30.

Wallace, L. A., Ott, W. R., and Weschler, C. J. 2015. Ultrafine particles from electric appliances and cooking pans: Experiments suggesting desorption/nucleation of sorbed organics as the primary source. *Indoor Air* 25: 536–546.

Weinhoffer, E. 2012. 3D printing FAQ. *Makezine*.Available at http://makezine.com/2012/11/15/makes-ultimate-guide-to-3d-printing-is-here/